A new hybrid immunocapture bioassay with improved reproducibility to measure tissue factor-dependent procoagulant activity of microvesicles from body fluids

Corentin Franco, Romaric Lacroix, Loris Vallier, Coralie Judicone, Tarik Bouriche, Sophie Laroumagne, Philippe Astoul, Francoise Dignat-George, Philippe Poncelet

A new hybrid immunocapture bioassay with improved reproducibility to measure tissue factor-dependent procoagulant activity of microvesicles from body fluids

Corentin Franco[1,4] (Corentin.franco@biocytex.fr), Romaric Lacroix[1,2] (Romaric.lacroix@univ-amu.fr), Loris Vallier[1,2] (Loris.vallier@gmail.com), Coralie Judicone[4] (Coralie.judicone@biocytex.fr), Tarik Bouriche[4] (Tarik.bouriche@biocytex.fr), Sophie Laroumagne[3] (Sophie.LAROUMAGNE@mail.ap-hm.fr), Philippe Astoul[3] (Philippe.astoul@ap-hm.fr), Francoise dignat-george[1,2] (francoise.dignat-george@univ-amu.fr), Philippe Poncelet[4] (Philippe.poncelet@biocytex.fr).

Authors' information:

1 Aix-Marseille Université, C2VN, UMR-1263, INSERM, INRA 1260, UFR de Pharmacie, Marseille, France.

2 Department of Hematology and Vascular Biology, CHU La Conception, APHM, Marseille, France.

3 Division of Thoracic Oncology, Pleural Diseases, and Interventional Pulmonology, Hôpital Nord, AP-HM, Marseille, France.

4 Research and Technology Department, BioCytex, Marseille, France.

Corresponding author: Prof. Françoise Dignat-George

C2VN, UMR-1263, INRA-1260, Faculté de Pharmacie, 27 Bd Jean Moulin, 13010 Marseille, France. E-mail address: francoise.dignat-george@univ-amu.fr.

Abstract

Background

The procoagulant activity of tissue factor-bearing microvesicles (MV-TF) has been associated with the risk of developing venous thrombosis in cancer patients. However, MV-TF assays are limited either by i) a lack of specificity, ii) a low sensitivity, or iii) a lack of repeatability when high-speed centrifugation (HS-C) is used to isolate MV. Therefore, our objective was to develop a new hybrid "capture-bioassay" with improved reproducibility combining MV immunocapture from biofluids and measurement of their TF activity.

Materials and Methods

Factor Xa generation and flow cytometry assays were used to evaluate IMS beads performance, and to select the most effective capture antibodies. The analytical performance between IMS-based and HS-C-based assays were evaluated with various models of plasma samples (from LPS-activated blood, spiked with tumoral MV, or with saliva MV) and different biofluids (buffer, plasma, saliva, and pleural fluid).

Results

Combining both CD29 and CD59 antibodies on IMS beads was as efficient as HS-C to isolate plasmatic PS+MV. The IMS-based strategy gave significantly higher levels of MV-TF activity than HS-C in tumor MV spiked buffer, and both pleural fluids and saliva samples. Surprisingly, lower TF values were measured in plasma due to TFPI (TF pathway inhibitor) non-specifically adsorbed onto beads. This was overcome by adding a TFPI-blocking antibody. After optimization, the new IMS-based assay significantly improved reproducibility of MV-TF bioassay versus the HS-C-based assay without losing specificity and sensitivity. In addition, this approach could identify the cellular origin of MV-TF in various biological fluids.

Conclusion

Compared to HS-C, the IMS-based measurement of MV-TF activity in body fluids improves reproducibility and makes the assay compatible with clinical practice. It can facilitate future automation.

KEY WORDS

Extracellular vesicle, Functional assay, Immunocapture, Microvesicle, Reproducibility, Tissue factor

INTRODUCTION

Stratification of patients according to their thrombotic risk remains a real challenge in various clinical settings such as cancer, cardiovascular disease, and immuno-inflammatory diseases. Current combinations of clinical and biological variables still fail to efficiently predict the risk of thrombosis arguing for a need for predictive biomarkers. Among the candidates, large extracellular vesicles (better known as microparticles or microvesicles, MV) are present in all biological fluids (blood, saliva, pleural effusions, etc.). They can promote coagulation and thrombosis (1–4). Indeed, MV provide a catalytic surface for the assembly of the coagulation complexes through 1) the exposure of anionic phospholipids such as phosphatidylserine (PS) on the external leaflet of the membrane and 2) the presence of tissue factor (TF), which is the main initiator of the coagulation cascade, on some subsets of vesicles (5–8).

The contribution of TF+ large extracellular vesicles (MV-TF) in thrombus formation (9–12) has been demonstrated in animal models using injection of exogenous MV from either leukocytes, endothelial cells, or tumor cells; it may also use endogenous production of cancer-derived MV. Moreover, prospective studies in cancer patients showed an association between elevated levels of MV-TF and the risk of developing venous thrombosis. However, the association between high levels of MV-TF and VTE has been shown in tumors with a high risk of thrombosis such as in glioblastoma and pancreaticobiliary cancer (13–16). This may be

78 due to a lack of sensitivity and reproducibility of the current methods used to measure MV-TF
79 in clinical samples as well as heterogeneous mechanisms involved in thrombus formation
80 according to the type of cancer and the cellular origin of the MV (17).

81 Assays currently available to measure MV-TF are based on different approaches—either
82 detecting the TF antigen on MV or measuring the TF-dependent procoagulant activity of MV.
83 Antigenic detection of TF on circulating MV shows limitations because 1) both cryptic and
84 decrypted TF may be equally detected whereas these two forms are not equally active and 2)
85 the measurement of TF by flow cytometry remains challenging because of its low levels on
86 MV (18,19). Alternative methods evaluate TF activity by measuring the capacity of MV to
87 generate factor Xa, thrombin, or a clot (20–23). In order to tackle specificity and sensitivity
88 issues related to such functional assays, we recently developed a new MV-TF activity assay
89 that includes a specific control based on an inhibitory anti-TF antibody (SBTF1) and involves
90 an optimized protocol (24) with improved specificity. However, the isolation process remains
91 a critical step. Indeed, when high-speed centrifugation (HS-C) is used for the isolation of MV
92 from plasma samples, variable activity levels are obtained with different rotors despite
93 standardization of the centrifugation protocol (time, speed, …); this leads to a lack of
94 reproducibility (24). Moreover, HS-C is known to generate MV aggregates impeding further
95 delineation of the cellular origin of the TF activity (25).

96 Beside this technical issue impeding the reproducibility of TF dependent MV assays, another
97 limiting condition is that none of them identify the cellular origin of MV-TF. The interest to
98 focus on specific subsets of MV-TF activity is supported by 1) the selective expression of TF
99 on endothelial, leukocytic, or tumor cell-derived MV and 2) the potential better predictive
100 value of MV subsets in regard to disease severity and cardiovascular complications(26).

101 Therefore, our objective was to develop a new assay, independent from HS-C, to improve the

repeatability of the current HS-C based assay (without losing specificity and sensitivity). Thus, immunomagnetic separation (IMS) was chosen as the MV isolation method. Our study shows that IMS offers efficient, repeatable, and selective measurement of MV-TF activity in various human body fluids (plasma, saliva, and pleural fluids).

MATERIALS AND METHODS

Biological fluid collection

Platelet-free plasma

Platelet-free plasma (PFP) were prepared from local blood bank donors, who signed an informed consent, being collected and processed according to the current minimal information for studies of extracellular vesicles guidelines(27). Briefly, blood was collected into 2.7 mL Vacutainer® tubes containing 0.109 mol/L sodium citrate (BD Diagnostics, Rungis, France) and incubated w/o lipopolysaccharide (LPS) (1 µg/mL, Escherichia coli O111: B4; Sigma Aldrich, Lyon, France) for 10 h at RT. The PFP was prepared with two successive centrifugations (2,500 g, 15 min, RT with a 5417R or C centrifuge -Rotor: F-45-30-11, Eppendorf, Montesson, France) and stored at -80°C until use.

Pleural fluids

Pleural effusion samples from cancer patients had been collected and processed as previously published(28). Briefly, they were centrifuged at 300 g for 10 min and at 1,000 g for 15 min at room temperature without stopping. The collected supernatant was stored at −80°C until further use. After thawing in a water bath at 37°C, a 1:10 dilution was necessary before measuring the MV-TF activity.

Saliva

Saliva samples (5 ml) were collected from healthy donors who did not eat or brush their teeth at least two hours before sampling. Samples were diluted 1:10 in buffer H (150 mM NaCl, 20

mM HEPES (4-(2-hydroxyethyl)-1-piperazine ethanesulfonic acid) and 0.1% NaN_3, pH 7.4, 0.22 µm filtrated) and centrifuged twice at 2500 g (15 min without a break) to remove cell debris before storage at -80°C until use. After thawing in a water bath at 37°C, an initial dilution of 1:3 was necessary before measuring MV-TF activity or for spiking experiments.

BxPC-3 and HAP-1 microvesicles preparation

Human adeno-pancreatic BxPC3 cells (Sigma Aldrich, Lyon, France) were cultured in RPMI 1640 medium (Thermo Fisher Scientific, Illkirch-Graffenstaden, France) supplemented with 10% fetal bovine serum (FBS), 1% penicillin, and 1% streptomycin (GIBCO BRL) in a humidified atmosphere at 37 C, 5% CO_2. Haploid human cell line (HAP1) and its TF knock-out derivative KO-TF-HAP1 were grown at 37°C and 5% CO_2 in Iscove's Modified Dulbecco's Medium (IMDM) supplemented with 10% FBS, 1% penicillin, and 1% streptomycin. Cell viability was assessed by trypan blue dye exclusion. TF-protein expression was checked by flow cytometry, and TF-gene expression was checked by qPCR. Cells were diluted 1:4 in new medium when they reached 80% confluence. The MV rich culture supernatant was cleared from cells by two successive centrifugations at 300 g for 5 min and from debris by centrifugation at 2,500 g for 15 min. Finally, MV were pelleted by HS-C at 24,000 g, 60 min, and washed twice in PBS-BSA (PBS BSA 0.1% - sodium azide 0.09%) before storage at -80°C until use. After thawing, MV were enumerated by flow cytometry as detailed below and spiked either in PFP or HEPES buffer.

Immunomagnetic beads preparation

Streptavidin beads selection

Streptavidin paramagnetic beads were selected according to the following criteria: a) a nominal size of 1 µm, b) a low non-specific capture of proteins, c) the absence of detergent in the final storage and reaction buffer, and d) a high level of free biotin binding per unit.

Antibody biotinylation

Many antibodies were used: CD4, CD11b, CD11c, CD13, CD14, CD15, CD18, CD24, CD29, CD30, CD33, CD38, CD41, CD43, CD45, CD45 RA, CD45 RO, CD46, CD48, CD52, CD54, CD55, CD59, CD61, CD62P, CD62L, CD63, CD64, CD66B, CD68, CD81, CD85j, CD86, CD89, CD98, CD99, CD101, CD115, CD131, CD146, CD162, CD326, anti-HLA-DR, and the irrelevant IgG1 control anti-DNP (Dinitrophenol). These were provided by Biocytex after being labeled as follows: antibodies were mixed with Sulfo-NHS-LC-Biotin (EZ-link/ThermoFischer, Illkirch-Graffenstaden, France) in amine-free PBS for 30 min at RT. Biotin-labeled antibodies and free biotin were separated using a desalting column in PBS (Sephadex G-25 in PD-10, GE Healthcare/Life Sciences, Tremblay-en-France, France). Positive fractions were concentrated with Amicon® Ultra-4 (Merck, Darmstadt, Deutschland) to obtain a final concentration of antibody higher than 1 mg/ml. Finally, biotinylated antibodies were stored in a conservation buffer at 4°C (PBS-Azide; 0.137 M NaCl, 0.27 mM KCl, 0.01 M Na_2HPO_4 18 mM KH_2PO_4, 0.09% sodium azide, pH: 7.4).

Coating and storage of streptavidin beads

Before coating, streptavidin beads were washed in PBS-BSA using a magnet bead separator (Dynamag-2, Invitrogen Dynal, Oslo, Norway). The beads were then incubated with the antibody solution during one min at RT. After removal of the supernatant, antibody-coated beads (IMS-beads) were washed in PBS-BSA buffer and stored at 4 mg/ml in the same buffer at 4°C.

IMS-based MV-TF activity assay

MV-TF activity was measured in samples either after isolation by HS-C as previously published (24) or by IMS as follows. Briefly, 100 µL of sample were incubated for 60 min at RT under mild rotative mixing. Different conditions of bead amount and contact time with

MV were tested as reported in the results section. The MV-loaded beads were washed and resuspended in 140 µl of HEPES buffer. The TF activity was then measured by a fluorogenic assay as described in Vallier et al. (24). Briefly, aliquots (70 µl) were pre-incubated for 30 min at 37°C with either an inhibitory anti-TF monoclonal antibody (10 µg/ml final, clone SBTF-1, BioCytex, Marseille, France) or a control antibody (10 µg/ml, clone a-DNP 2H11-2H12, BioCytex, Marseille, France). Then, 8 µl HEPES-Ca^{2+} buffer (150 mM NaCl, 20 mM HEPES and 0.1% NaN_3, 50 mM $CaCl_2$, pH 7.4, 0.22 µm filtrated) containing purified human FVII and FX (Stago BNL, JV Leiden, Netherland) was added to each 70 µl sample to produce final concentrations of 10 nM, 190 nM, and 5 mM $CaCl_2$ respectively and incubated for another 2 h at 37°C. FXa generation was stopped by the addition of 8 µl of EDTA buffer (150 mM NaCl, 20 mM HEPES and 0.1% NaN_3, 200 mM EDTA, pH 7.4, 0.22 µm filtrated). To avoid beads interference, the supernatant was transferred in another plate after magnetization of beads. The FXa fluorogenic substrate (1 mM final, BioCytex, Marseille, France) was added onto the bead supernatant. Finally, the fluorescence at 390 nm (excitation) and 460 nm (emission) was monitored for 15 min at 37°C on a microplate fluorescence reader (Fluoroskan, CAT instrument, Stago, Asnières-sur-Seine, France). Data from plasma-purified MV were expressed as fmol/L by comparison to a calibration curve generated using recombinant TF. Irrelevant IMS were performed using beads coated with an antibody against DNP—a small hapten molecule not expressed on human cells.

Flow cytometry analysis

Microvesicle gating

MV were analyzed by flow cytometry on a last generation instrument (CytoFLEX S*, Beckman Coulter) in which the side scatter (SSC) parameter was collected at 405 nm (violet SSC) to improve the size-related resolution in the sub-micron range. A standardized gate for

MV analysis was determined with the help of a new tool called Gigamix-Plus (BioCytex) made of eight different polystyrene beads (75 nm, 100 nm, 160 nm, 200 nm, 240 nm, 300 nm, 500 nm and 900 nm) obtained by mixing both Megamix-Plus SSC and FSC beads (29), and supplementing by an additional 75 nm bead. We set the MV gate using Gigamix-Plus in comparison to Megamix-Plus SSC as described in detail in Supplemental Figure 1. Briefly, the lower limit is defined under the 75 nm beads and the upper limit is over the 900 nm beads.

Microvesicle enumeration

Samples (10 µl) containing MV were incubated 15 min at RT with a mixture of 0.7 µl of Annexin V-FITC (fluorescein isothiocyanate) 1:30 in calcium buffer (Tau Technology, Kattendijke, NL), 0.7 µl CD235a-AF735 (Alexa Fluor735, 11E4B-7-6, Beckman-Coulter), 0.7 µl CD15-BV650 (brilliant violet 650, W6D3, Biolegend Saint-Cyr-l'École, France), and 0.5 µl CD41-PE (phycoerythrin, PL2-49**,** Biocytex) or 0.5 µl of HLA DR-PE (Immu-357, Beckman Coulter) in 100 µl calcium buffer. The positivity threshold was determined beforehand with isotype controls matched with their relevant antibody conjugates in terms of fluorescence background. The MV subsets were defined as follows: platelet-MV (PMV) as AnnV+/CD41+, erythrocyte-MV (EryMV) as AnnV+/CD235a+, granulocyte-MV (GranMV) as AnnV+/CD15+, monocytes-MV (and few B lymphocytes-MV) (HLA-DR MV) as AnnV+/HLA-DR+, and epithelial cancer MV as AnnV+/CD326+. When needed, absolute counts of MV were determined using MP-Count Beads (BioCytex) as previously published (30).

Statistical analysis

Statistical analyses were performed with GraphPad Prism software version 5.0 (GraphPad Software, San Diego, CA, US). Significant differences were determined using a non-

parametric Mann-Whitney test and one-way ANOVA. A p-value less than 0.05 was considered statistically significant.

RESULTS

Comparison of IMS and high-speed centrifugation to isolate MV from plasma

To select the best immuno-magnetic tools to isolate MV from body fluids, we first evaluated the MV capture efficiency of several magnetic beads coated with various antibodies. This was achieved by counting the remaining MV detectable by flow cytometry in plasma samples post-IMS. Figure 1A illustrates a few examples of isolations by beads coated with antibodies against CD55, CD15, CD41, and anti-HLA-DR. Either all PS+ MV (AnnV+ MV) or the specifically targeted subsets Gran-MV (CD15+), PMV (CD41+) or Mono- (+/- B Lymphocytes, HLA-DR+) MV were removed.

The performance of IMS in depleting MV from various subtypes is reported in Table 1. Non-specific depletion with Ctrl-IMS was minimal (<5%). IMS-based MV isolation depended on the beads' specificity. Lineage-oriented magnetic separations were efficient to remove their respective targets: CD41-coated beads removed 98+/-3% of PMV, CD15 beads removed 92+/-4% of Gran-MV, and anti-HLA-DR-coated beads removed 84+/-15% of Mono-MV. The non-specific capture induced by unreactive beads (a-DNP IMS) remained low (< 5%). The non-specific capture of untargeted MV subsets in lineage-oriented IMS systems was sometimes surprisingly higher than expected (up-to 35%) and was mainly observed when the most frequent PMV subset was targeted using CD41 IMS. In our hypothesis, the highest levels of non-specific capture might be due to the co-isolation of aggregated vesicles, e.g., CD15+ Gran-MV aggregated with CD41+ PMV may come out with CD41 IMS.

However, each of these individual bead types captured significantly less FCM-characterized PS-expressing MV (AnnV+ MV) than what HS-C could isolate. Therefore, these could not replace HS-C for exhaustive capture. Even beads targeting widely represented antigens (CD29, CD55, CD59, and HLA-ABC) provided a significantly lower percentage of isolation than HS-C. Thus, a combination strategy was tested where the same beads were coated with two different antibodies with synergistic antigenic coverage (CD29-59 IMS). Figure 1B and Table 1 show that CD29-59 IMS could isolate as many AnnV-MV as HS-C (84+/-7% *vs* 82+/-10%, respectively, p = 0.7). CD29-59 IMS and HS-C displayed the same efficiency to isolate CD41, CD15, and HLA DR MV from plasma and was significantly more efficient to capture the CD235a+ (erythrocytic) MV. The CD29-59 beads were therefore selected as an appropriate tool to replace centrifugation.

Comparison of CD29-59 IMS and high-speed centrifugation based MV-TF activity assays in different body fluids

The efficacy of CD29-59 IMS to isolate the MV-TF activity was tested on different body fluids, by reference to HS-C. Figure 2A shows that when using CD29-59 IMS rather than HS-C, TF activity levels were significantly increased for saliva (+53% +/-5.3%, p=0.007) and for tumoral pleural effusions (+84 +/-4.7%, p=0.016). Similarly, significantly more MV-TF activity was measured when tumoral MV (BxPC3 MV) was spiked in HEPES buffer. However, the IMS-based activity dropped when the same amount of MV was spiked in plasma suggesting that a soluble plasma component interfered with this measurement. Thus, we tested the hypothesis that TFPI (tissue factor pathway inhibitor: the major plasmatic inhibitor of TF) may be adsorbed on the plastic beads rather than be washed-out after IMS. A range of TFPI concentrations (0-1500 ng) was incubated on unspecific IMS beads (Ctrl-IMS) in HEPES buffer. After 60 minutes, Ctrl IMS beads were washed and incubated with BxPC-3 MV. As a result, we observed a dose-dependent inhibition of the MV-TF activity starting from the infra-physiological TFPI concentration of 6.2 ng/ml (Figure 2B).

As confirmed in Figure 2C, the MV-TF activity was inhibited when IMS beads were pre-incubated in normal plasma (NP) but was preserved using TFPI-deficient plasma (DEF) or in the presence of an anti-TFPI antibody. Altogether, these results demonstrate that plasmatic TFPI is adsorbed by the IMS beads and is responsible for the decrease of MV-TF activity isolated from plasma. Therefore, the anti-TFPI antibody was systematically incorporated into the IMS-based assay, and also into the HS-C-based assay for future comparisons.

Optimization of IMS conditions for measuring MV-TF activity.

To optimize the IMS conditions, we next varied the concentration of beads and the time of MV capture. MV-TF activity was measured in plasma samples prepared from LPS-treated whole blood. Figure 3A shows that a minimum amount of 3N (N=33 µg) CD29-59 beads was required to get significantly increased MV-TF activity versus HS-C (+33% +/-3%, p = 0.0132). No significant increase was found upon further increasing the amount of beads; thus, 3N was selected as the adequate quantity. Using this amount of beads, we next defined the optimal time of capture to be 60 min (Figure 3B). Interestingly, increasing the amount of beads (6N) could reduce this time down to 30 min. However, the condition 3N x 60 min was selected as the best compromise between cost and IMS-based isolation efficiency for further experiments. These chosen IMS conditions were robust to the amount of total MV present in the sample. Indeed, as illustrated in Suppl Fig. 2, the MV-TF activity could be efficiently isolated even in a large excess of total MV in the sample after spiking LPS-activated plasma with MV from saliva and increasing the total load of MV more than 10-fold.

Of note, these same IMS conditions were also verified to deplete more than 95% of the TF antigen present in a suspension of washed BxPC3 MV as illustrated in Suppl. Fig. 3; HS-C still left about 10% of MV-associated TF in the supernatant.

Evaluation of analytical performance of the IMS-based MV-TF activity assay

We then evaluated the sensitivity, specificity, linearity and reproducibility of the optimized IMS assay in various models of platelet-free plasma. First, in the BxPC3 MV-spiked plasma model, we showed that TF-PCA was significantly increased using IMS versus HS-C (67+/-4.0 fM *vs* 13+/-7.0 fM; p<0.0001, n= 9; Figure 4A). This increased sensitivity was confirmed while studying the other model of plasma from LPS-activated versus unstimulated blood (Figure 4B), even in the lower range of MV-TF concentrations measured in normal plasma (10+/-1.3 fM *vs.* 4.0+/-2.7 fM; p=0.002). Second, the TF specificity of the IMS-based assay was checked using MV (HAP-MV), which had TF knocked-out. Figure 4C shows that no TF-specific activity was measured over a wide range of concentrations of KO-TF-HAP MV in contrast to parental MV (HAP-MV), confirming the specificity of the assay. Third, the test had good linearity using the same MV (r^2> 0.99; Figure 4D).

The quantity of IMS beads used in our MV isolation protocol should not only be optimal for normal plasma but should also be applicable in a pathological context associated with high amounts of MV. This was checked with a model of plasma spiked with excess amounts of saliva MV. Indeed, our system maintained a comparable MV isolation capacity despite the addition of more than 10 times the amount of total MV present in unspiked plasma. (Supplemental Figure 2).

Finally, we compared IMS and HS-C (Table 2) in terms of reproducibility. The coefficient of variation (CV) for repeated assays was lower using IMS than HS-C in low, medium, and high ranges of activity (mean value: 9% +/-5% *vs* 25% +/-10%, p=0.05). Similarly, the inter-operator reproducibility was significantly improved in the IMS condition (CV mean value: 12% +/- 5.5% *vs* 28% +/- 11%, p=0.04). These results showed the better reproducibility of the CD29-59 IMS-based MV-TF activity assay versus the HS-C-based version without losing the sensitivity and TF specificity of the assay.

Identification of the origin of MV-TF by selective IMS

One theoretical advantage of immunological capture is to help identify the cellular origin of MV-TF. Thus, we performed multiple selective IMS made to capture MV subsets on plasma from LPS-activated blood (LPS-plasma) and cancer pleural fluids. A case of LPS-plasma is illustrated in Figure 5A featuring an initial screening of forty putative target antigens including platelet-, endothelium- and leucocyte-associated markers; mostly monocyte-associated markers were chosen here because of the well-known TF-inducing effect of LPS activation on monocytes.

IMS experiments were stratified according to the level of isolated TF activity. Figure 5A shows a broad range of TF activity levels depending on the specificity of the antibody coated on the IMS beads. IMS isolations with an activity <5 fM TF were considered negative including those targeting the platelet-, endothelium-, and granulocyte-lineage specific antigens CD41, CD61, CD62P, CD146, and CD66b. In contrast, some IMS beads were isolated with high activity levels (~ or > 50 fM), which is comparable to that of our previous "Pan MV" reference CD29-59 IMS, i.e., CD11b, CD18, anti-HLA-DR, CD33, and CD45. Interestingly, most other IMS beads tested, targeting well-known monocyte-associated antigens such as CD14, CD64, CD11c, CD13, CD38, CD4, CD54, and CD162, collected lower albeit clearly significant levels of activity (10-50 fM TF). This suggests a monocytic origin of the TF-PCA in this sample (Fig. 5A).

A new experiment (Fig. 5B) clearly confirmed this preferential monocytic orientation. Other than the anti-HLA-DR IMS that recovered the same high level of activity as the "pan-MV" CD29/59 IMS, the gran-MV-oriented CD15 IMS, the PMV-oriented CD41 IMS, and the endo-MV-oriented CD146 IMS all captured negligible levels of TF activity.

We similarly studied the MV-TF activity in the case of cancer pleural effusion (Fig. 5C). This was mainly supported by MV showing the positivity for CD326, i.e., the epithelial cell adhesion molecule (EpCAM)—an antigen over-expressed on most solid tumors. In addition to CD326 IMS, significant levels of TF-PCA were also isolated from this single example of pleural fluid using anti-HLA-DR as well as CD146 IMS suggesting the presence of TF+/HLA-DR+ monocyte MV (MonoMV) as well as TF+/CD146+ Endo-MV or the co-expression of these antigens (EpCAM/CD326, HLA-DR and MCAM/CD146) on the same Tumor-MV. Thus, IMS allowed the use of a large library of specificities and was a useful tool to investigate the cellular origin of the MV-TF activity in biological samples.

DISCUSSION

Here, we developed a new hybrid capture bioassay to measure MV-TF activity that bypasses HS-C to isolate MV from human body fluids. The novelty of this assay is that it combines the specific immunocapture of MV from body fluids with the measurement of TF activity. The use of magnetic beads coated with both anti-CD29 and anti-CD59 antibodies is as efficient as HS-C to isolate all PS+ MV detectable by flow cytometry. It is more efficient than HS-C to recover the MV-associated TF activity. The use of several body fluids (plasma, pleural fluid, and saliva) demonstrated that the new assay was more reproducible than the HS-C-based assay without losing sensitivity and TF specificity. Moreover, we showed for the first time that IMS can identify the cellular origin of MV-TF in biological samples.

Whole plasma (or even whole blood) coagulation assays have been proposed to measure TF-dependent procoagulant activity (TF-PCA)(8,31,32). Although each of the TF activity assay principles has its own advantages and limitations, global assays are most often dependent on

inhibitors such as TFPI, clotting factors other than TF, or on-going treatments(33) such as heparin(32) or oral anti-coagulants. Such assays are also affected by non-TF-dependent alternative coagulation systems such as the contact pathway. These assay principles may need blockage with CTI or anti-FXI antibodies(31,32) to neutralize the contribution of the contact pathway and they often create complex result interpretation.

In contrast, our approach avoids interferences by first isolating TF-bearing MV from their plasmatic environment and then using synthetic systems to reveal TF activity as already described for FXa generation assays. Indeed, most whole plasma methods such as the fibrin generation test(32) also use MV isolated from patient samples followed by spiking into a well-known matrix of MV-free normal plasma pool. Thus, even with whole plasma or blood clotting assays, MV isolation prior to TF-PCA evaluation looks like a mandatory step as shown by Aras et al(34).

Different methods have been described in the literature to isolate small or large extracellular vesicles (EV) from various biological fluids (35,36). Among methods based on physical properties of MV, density gradient separation and especially flotation result in a good purity of EV but are very time-consuming with generally low and non-reproducible yields (37,38). Polymer-based isolation mainly including poly-ethylene glycol (PEG) precipitation is fast but shows a high level of non-EV contamination (37,38). Size exclusion chromatography (SEC) is a good compromise between yield and purity but necessitates sample re-concentration after elution and is not compatible with clinical practice (39,40). Centrifugation, either “high-speed” (HS-C i.e. ~20,000 g) for large EV (MV) or ultra-centrifugation (> 70,000 g) for small EV is the most commonly used method for isolating EV; however, centrifugation is time-consuming andprovides EV with low recovery, low purity (41–43) and limited reproducibility (24). Immunological approaches based on target antigen(s) expression can use FACS to specifically isolate large EV, but ththis is time-consuming and requires expensive and

complex equipment (44). Microfluidic techniques (45) based on immuno-capture of EV in micro-channels can be specific, but they may also be characterized by low recovery yields due to a limited binding capacity.

By illustrating IMS in biological fluids other that plasma samples, we demonstrate here that this new approach 1) can be applied in various body fluids regardless of the viscosity of the medium and 2) that its efficacy is as good as high speed centrifugation (HS-C). Indeed, media viscosity is a critical parameter that influences the efficiency of EV isolation for most EV isolation techniques. Importantly, IMS may be one of the least influenced isolation methods because affinity binding rather than physical properties of EVs are the main drivers. Indeed, IMS as an isolation technology for e.g. cells or bacteria, has been applied in complex biological samples such as whole blood, bone marrow, and even stool samples. Thus, it appears to be the most appropriate for viscous media.

We showed here that the new IMS strategy was as efficient as HSC to isolate MV. Indeed, the use of magnetic beads coated with antibodies with broad specificity allows exhaustive capture of target antigen-positive MV probably due to the large binding surface provided by microspheres ensuring high probability of meeting between MV and beads. IMS has already been used to isolate either i) most EV via targeting broadly represented molecules or ii) subsets of EV using lineage-specific antigens. First, phosphatidylserine (PS) was targeted to isolate EV using beads coated with annexin V or TIM-4 (T-cell membrane protein 4) in a calcium-dependent manner or with lactadherin (46,47) as a calcium-independent alternative. However, PS is not expressed on all EV (48). Tetraspanins (CD9, CD63, and CD81) are the most frequently targeted antigen to isolate EV (49) but these specificities are mostly related to small EV and may not cover all EV especially the procoagulant TF-positive MV that we aim to collect. We used a screening strategy based on numerous cell-surface CD to show that the combined targeting of both CD29 and CD59 antigens was an effective strategy to isolate most

MV in general as seen in FCM and most TF activity-bearing MV in particular. This potential was probably due to their broad and complementary expression on circulating cells and also MV. Indeed, CD59/MIRL serves as a complement decay ecto-enzyme and must be present on all nucleated cells as well as on red blood cells at a significant level (e.g. 45,000 molecules/RBC (50)) since its absence is pathological, e.g. in paroxysmal nocturnal hemoglobinuria (51). We also considered this to be an attractive target since its GPI anchorage appears favorable for its association with lipid rafts and thus its incorporation onto EV membrane (52,53). Integrins are also known to be well expressed on MV (54) and CD29—these are common beta chains of all very late activating antigen (VLA; CD49 a to f) and can be found on many leucocytes. This glycoprotein is also present on platelets as part of the GPIa/IIa complex; thus, it complements the low expression of CD59 on platelet (and PMV) surfaces.

Compared to HS-C, our IMS strategy was more sensitive to recovering the MV-associated TF activity. Indeed, the MV-PCA was higher in the IMS assay than the HS-C in tumor MV-spiked buffer, saliva, and pleural fluids. The apparent decrease observed in plasma was due to a nonspecific adsorption of TFPI onto beads—this decrease was overcome by adding a TFPI blocking antibody. The addition of anti-TFPI in thrombin generation assays increases the activity already reported (55). This addition is a major difference with the previous HS-C version of the assay (24) and asks whether the information obtained by the two types of assays is of similar nature given the pathophysiological role of TFPI. However, previous observations questioned the HS-C process around 20,000 g and the subsequent EV washing already removed the soluble TFPI while higher centrifugation speeds (>70,000 g) retained it (24). In agreement with that, the conditions of the HS-C-based MV-TF activity assay (24,000 g, 1 h x 2) showed no significant difference with or without the presence of TFPI-neutralizing antibody (data not shown). Thus, both the HS-C and IMS versions of the MV-TF assays

458 measure similar information. Therefore, better sensitivity of the new IMS-based assay in
459 comparable volumes (i.e. 100 µL) of plasma should be attributed to a better level of MV
460 capture rather than to the inhibition of TFPI because we demonstrated an exhaustive (>95%)
461 immune-depletion of the MV-associated TF antigen whereas HS-C left about 10% in the
462 supernatant (illustrated in Suppl. Fig. 3).

463 This higher sensitivity of CD29-59 IMS versus HS-C was demonstrated by 1) the existence of
464 a basal level of MV-TF activity that was much higher in unstimulated PFP from healthy
465 donors and by 2) the significant increase of activity for MV in LPS-stimulated PFP. The
466 higher sensitivity of the new IMS-based assay is probably due to a better level of MV capture
467 especially the smallest ones that express TF and PS but remain below the detection threshold
468 of the most sensitive flow cytometry protocol.

469 The most important technical advance of our new hybrid TF assay is to bypass HS-C to
470 isolate MV. Indeed, we have previously shown that isolation of the MV by HS-C has limited
471 reproducibility and repeatability as shown by the CV of MV TF activity data: These metrics
472 were significantly improved by bypassing centrifugation (56). This limited reproducibility
473 associated with HS-C is consistent with previous studies showing that the recovery of the
474 pellet depends on the rotor type, the centrifugation speed (g-force), and the centrifugation
475 time (57): These are physical parameters that were shown to significantly affect MV TF
476 activity (56). Other disadvantages of centrifugation are the induction of MV aggregation (36)
477 and the failure to discriminate MV from contaminating structures such as protein/lipid
478 aggregates (35); both of these are responsible for limited purity. Here, we show that the use
479 magnetic beads is an option to overcome the disadvantages of centrifugation and can
480 specifically reducing the time to isolate MV and avoid washing steps.

481 As we first showed in Cointe et al. (58), IMS was more reproducible than HS-C to evaluate

the fibrinolytic capacity of CD15 + MV in septic patients (58). This work similarly shows a major improvement brought into this PCA assay, i.e, lower CVs measured for intra-assay repeatability (mean value: 9% +/-5% *vs* 25% +/-10%, p=0.05; Table 2). Also, the inter-operator reproducibility was significantly improved in the IMS condition (CV mean value: 12% +/- 5.5% *vs* 28% +/- 11%, p=0.04). This reproducibility was not obtained at the expense of sensitivity nor TF specificity. This increase is likely because IMS requires minimal hands-on time and produces purified MV enabling downstream analysis.

Although intrinsic assay performance seems encouraging, the clinical interest of this new IMS-based MV-TF activity assay to predict thrombosis remains to be evaluated. The potential of this assay format using IMS for automation on laboratory robots should even enable better robustness for future routine use. Interestingly, it will have value in both plasma and other biofluids.

Moreover, we showed that IMS can provide an opportunity to identify the cellular origin of MV-TF in biological samples. We first used a well-known model in the field where in vitro LPS activation of whole blood induces i) de novo TF expression on the surface of monocytes (59) as well as ii) TF PCA in plasma derived from the activated blood. Our study involved a screening strategy with numerous cell-surface targets (CD) including or lineage-specific or lineage-associated antigens (e.g., monocyte-associated antigens). We found that most of these specificities could isolate significant TF activity. This confirmed the expected monocytic origin of MV-TF activity in plasma from LPS-activated blood. The fact that targeting these monocyte-associated markers isolated different levels of activity may be linked to variations in i) antigen density on monocyte-derived TF+EV and ii) monoclonal antibody affinity. In contrast, all IMS isolations directed against antigens specific for other MV subsets were negative including those against Gran-MV (CD15, CD66b), Endo-MV (CD146), and PMV (CD41, CD62P) with CD61 being possibly shared between PMV and EMV(60)

507 The new IMS strategy was also useful to define the cellular origin of MV-PCA in pleural
508 fluid sample as illustrated for a case of EpCAM-positive epidermoid cancer. Indeed, CD326+
509 tumor-MV could be detected in this fluid illustrating that specific IMS isolation of EV
510 included into a bioassay provides useful information to delineate the tumor cell origin of the
511 MV-TF activity.

512 IMS has been previously used to isolate specific tumoral subsets using glypican-1 (61) to
513 identify cancer exosomes, EpCAM to detect epithelial cancers (62,63), EGFRv3 to capture
514 glioblastoma-derived small EV (64), CSPG4 to detect patients with melanoma (65), and CA-
515 125 to detect ovarian cancer (66). However, none of these IMS-based approaches were
516 intended to quantify a functional activity on EV.

517 Thus, measuring MV-TF activity using IMS isolation is an innovative approach that tackles
518 the issue of HS-C reproducibility without losing sensitivity or TF specificity and gives access
519 to the determination of TF-PCA on MV subpopulations. These crucial improvements make
520 the measurement of MV-TF activity more compatible with clinical practice and open the way
521 for future automation.

522

523 # Tables

		All MV	PMV	EryMV	GranMV	HLADR MV
	HS-C	82±10	91±9	43±16	87±5	82±10
	Ctrl IMS	3±3	5±7	0	2±7	3±2
Lineage specific antigens	**CD41 IMS**	50±13	98±3	19±16	33±36	23±27.2
	CD15 IMS	22±11	18±16	0	92±4	22±20
	HLA-DR IMS	27±6	13±11	0	19±14	84±15
Widely represented antigens	**CD29 IMS**	58±17	93±3	11±17	41±22	78±10
	CD55 IMS	49±16	63±21	55±26	52±20	59±20
	CD59 IMS	48±28	52±33	66±45	70±25	47±20

	HLA-ABC IMS	66±13	83±9	23±23	75±10	75±17
	CD29-59 IMS	84±7	97±3	83±10	91±1	89±4

Table 1. Efficacy of MV depletion as measured by high sensitivity flow cytometry.

Three platelet-free plasma (PFP) samples from three patients were treated with i) a high-speed centrifugation (HS-C) or ii) an IMS-based isolation protocol (different specificities were used). The results indicate the percentage of microvesicle (MV) depletion in each sub-population compared to the original sample (reference for 0% depletion). Grey shading indicates that MV depletion is better than or equal to HS-C. The various gates of interest in the flow cytometry protocol were defined via labeling with Annexin V-FITC ("All MV"), CD41-PE (PMV), CD235a-AF750 (EryMV), CD15-BV650 (GranMV), and anti-HLA-DR-PE (Mono and B-lymphocyte-MV). HS-C: high-speed centrifugation; Ctrl IMS: A non-reactive antibody was coated on the IMS beads.

	Sample	**MV-TF level**	**MV isolation**	**Number of samples**	**Number of operators**	**CV (%)**
Repeatability 1	BxPC-3 PFP	High	HS-C	3	1	37
			CD29-59 IMS	3	1	1.2
Repeatability 2	LPS-act. PFP	Medium	HS-C	3	1	20
			CD29-59 IMS	3	1	8.1
Repeatability 3	Unstim. PFP	Low	HS-C	3	1	19
			CD29-59 IMS	3	1	17
Inter-operator reproducibility 1	BxPC-3 PFP	High	HS-C	3	3	35
			CD29-59 IMS	3	3	10
Inter-operator reproducibility 2	LPS-act. PFP	Medium	HS-C	3	3	16
			CD29-59 IMS	3	3	7
Inter-operator reproducibility 3	Unstim. PFP	Low	HS-C	3	3	33
			CD29-59 IMS	3	3	18

Table 2. Comparison of reproducibility between optimized IMS- and HS-C-based MV-TF assays. BxPC-3 PFP: MV BxPC-3 spiked into PFP, unstimulated PFP (Unstim PFP) and LPS-activated plasma (LPS-act. PFP). HS-C: high-speed centrifugation; IMS: immunomagnetic separation.

Figure legends

Figure 1: IMS-based MV isolation depends on the beads' specificity. A. Flow cytometry-based quantitation of residual MV before and after depletion with IMS (Immunomagnetic separation) or centrifugation. All results were obtained on CytoFLEX®, and actual events were previously gated on VSSC-H (violet side scatter height) using a Gigamix-Plus strategy. The various gates of interest were defined by labelling with Annexin V-FITC (All MV), CD15-BV650 (GranMV), CD41-PE (PMV), and HLA-DR-PE (Mono and B lymphocyte - MV). In a representative experiment, the last column shows the absolute number of MV remaining after isolation in supernatants (SN) in the same sample volume, i.e. MV not collected by CD55 IMS beads (among all AnnV+ MV), CD15 IMS beads (among CD15+ MV), CD41 IMS beads (among CD41 MV), and anti-HLA-DR IMS beads (among HLA-DR+ MV). B. The depletion efficiency for each MV subset is compared between high-speed centrifugation (HS-C) and CD29-59 IMS (mean+/-s.d. values from three different platelet-free plasma). NS: $p>0.05$; *: $p<0.05$.

Figure 2: Comparison of CD29-59 IMS-based and high-speed centrifugation-based MV-TF activity assays in different body fluids and the impact of TFPI

A. Comparison of yields between centrifugation (HS-C, 100%) and CD29-59 IMS in saliva (n=6), pleural fluids (n=4), HEPES buffer, or plasma samples spiked with purified cancer MV-TF (n=4). **B.** Inhibition of MV-TF activity by non-specific adsorption of TFPI on IMS beads. A wide range of TFPI concentrations (0-1500 ng) in HEPES buffer was added on a-DNP Mab-coated (sham-) IMS beads. After 60 minutes, sham-IMS beads were washed and incubated with BxPC-3 MV before measuring the MV-TF activity. The physiological plasmatic concentrations of TFPI are indicated in the graph as "TFPI normal values" **C**. Efficacy of anti TFPI (α-TFPI) to neutralize the inhibitory effect of TFPI on MV-TF activity. MV-TF activity was measured on BxPC3 MV in the absence or presence of sham-IMS beads (μS) previously incubated with normal plasma (NP), TFPI-immunodepleted plasma (DEF), or NP with anti-TFPI antibody. Each sample (n) was treated in triplicate. NS: $p>0.05$; *: $p<0.05$;**: $p<0.01$; and ***: $p<0.001$.

Figure 3: Optimization of experimental conditions in the bead-based MV-TF activity assay. The amount of beads and incubation time were key factors to optimize when outperforming the centrifugation-based isolation method **A.** N to 4N amounts of CD29-59 IMS beads (white bars) were compared to high-speed centrifugation (Grey bar, HS-C, 100%) on 100 µl of PFP from LPS-activated blood. The activity levels after IMS isolation were compared to those gained via centrifugation. **B.** 3N (white bars) and 6N (dark grey bars) show the amount of CD29-59 IMS beads tested at 15, 30, 45, and 60 min and compared to high-speed centrifugation (grey bar, HS-C, 100%) (2 x 60 min 24000 g) (mean values from triplicates). NS: $p>0.05$; *: $p<0.05$; **: $p<0.01$; and ***: $p<0.001$.

Figure 4: Comparison of analytical performance between optimized IMS- and HS-C-based MV-TF assays. A and B. Sensitivity. MV-TF activity was measured on BxPC-3 MV spiked into PFP (A) (n=9 i.e. 3x3 performed by 3 different operators) or (B) on 11 PFP w/o

LPS stimulation. C. Specificity. MV-TF activity was measured on HAP1- (grey bars) and KO-TF-HAP1- (white bars) MV spiked in PFP. Ctrl IMS: IMS beads coated with an irrelevant antibody (anti-DNP). The dotted line represents the limit of quantification. (n=3) D. Linearity. MV-TF activity was measured on HAP1-MV spiked in PFP at various levels (n=3). HS-C: high-speed centrifugation; IMS: immunomagnetic separation. **: $p<0.01$ and ***: $p<0.001$.

Figure 5: Selection of an effective panel of monoclonal antibodies to identify the pro-coagulant subpopulations of MV in the LPS model and an example of cancer pleural fluid (A) Results of multiple IMS isolations of MV-TF activity (vs. centrifugation as a reference). CD29-59 reference IMS (Grey bar). (B) Immunocapture of different MV subsets compared to CD29-59 IMS in the LPS model. (C) Immunocapture of different MV subsets compared to CD29-59 IMS in a sample of cancer pleural fluid (values from triplicates).

Funding sources

C.F. was supported by ANRT (Association Nationale de la Recherche et de la Technologie) in the context of the CIFRE system.

Declaration of Competing Interest

We disclose as a conflict of interest that P. P, T. B, and C. J are full-time employees of Biocytex. F. DG and R.L disclose grants from Stago and a patent on microvesicle fibrinolytic activity licensed to Stago.

Citations

1.R. Lacroix, L. Vallier, A. Bonifay, S. Simoncini, D. Mege, M. Aubert, L. Panicot-Dubois, C. Dubois and F. Dignat-George, Microvesicles and Cancer Associated Thrombosis, *Semin. Thromb. Hemost.* **45** (2019) 593–603.; DOI:10.1055/s-0039-1693476

2.A.-L. Ståhl, K. Johansson, M. Mossberg, R. Kahn and D. Karpman, Exosomes and microvesicles in normal physiology, pathophysiology, and renal diseases, *Pediatr. Nephrol. Berl. Ger.* **34** (2019) 11–30.; DOI:10.1007/s00467-017-3816-z

3.S. Nomura, M. Niki, T. Nisizawa, T. Tamaki and M. Shimizu, Microparticles as Biomarkers of Blood Coagulation in Cancer, *Biomark. Cancer* **7** (2015) 51–56.; DOI:10.4137/BIC.S30347

4.Y. Chen, G. Li and M.-L. Liu, Microvesicles as Emerging Biomarkers and Therapeutic Targets in Cardiometabolic Diseases, *Genomics Proteomics Bioinformatics* **16** (2018) 50–62.; DOI:10.1016/j.gpb.2017.03.006

5.A. P. Owens 3rd and N. Mackman, Microparticles in hemostasis and thrombosis, *Circ. Res.* **108** (2011) 1284–1297.; DOI:10.1161/CIRCRESAHA.110.233056

6.R. F. A. Zwaal and A. J. Schroit, Pathophysiologic Implications of Membrane Phospholipid Asymmetry in Blood Cells, *Blood* **89** (1997) 1121.; DOI:PMID: 9516159

7.N. Satta, F. Toti, O. Feugeas, A. Bohbot, J. Dachary-Prigent, V. Eschwège, H. Hedman and J. M. Freyssinet, Monocyte vesiculation is a possible mechanism for dissemination of membrane-associated procoagulant activities and adhesion molecules after stimulation by lipopolysaccharide, *J. Immunol. Baltim. Md 1950* **153** (1994) 3245–3255.; DOI:PMID: 7522256

8.S. Butenas, B. A. Bouchard, K. E. Brummel-Ziedins, B. Parhami-Seren and K. G. Mann, Tissue factor activity in whole blood, *Blood* **105** (2005) 2764.; DOI:10.1182/blood-2004-09-3567

9.J. L. Yu, L. May, V. Lhotak, S. Shahrzad, S. Shirasawa, J. I. Weitz, B. L. Coomber, N. Mackman and J. W. Rak, Oncogenic events regulate tissue factor expression in colorectal cancer cells: implications for tumor progression and angiogenesis, *Blood* **105** (2005) 1734–1741.; DOI:10.1182/blood-2004-05-2042

10.M. Davila, A. Amirkhosravi, E. Coll, R. D. Liza and J. Francis, Tissue Factor-Bearing Microparticles Derived from Tumor Cells: Impact on Coagulation Activation., *Blood* **108** (2006) 1757–1757.; DOI:10.1182/blood.V108.11.1757.1757

11.S. Falati, Q. Liu, P. Gross, G. Merrill-Skoloff, J. Chou, E. Vandendries, A. Celi, K. Croce, B. C. Furie and B. Furie, Accumulation of tissue factor into developing thrombi in vivo is dependent upon microparticle P-selectin glycoprotein ligand 1 and platelet P-selectin, *J. Exp. Med.* **197** (2003) 1585–1598.; DOI:10.1084/jem.20021868

12.E. Ramacciotti, A. E. Hawley, D. M. Farris, N. E. Ballard, S. K. Wrobleski, D. D. Myers Jr, P. K. Henke and T. W. Wakefield, Leukocyte- and platelet-derived microparticles correlate with thrombus weight and tissue factor activity in an experimental mouse model of venous thrombosis, *Thromb. Haemost.* **101** (2009) 748–754.; DOI:PMID: 19350121

13.F. J. S. H. Woei-A-Jin, M. E. T. Tesselaar, P. Garcia Rodriguez, F. P. H. T. M. Romijn, R. M. Bertina and S. Osanto, Tissue factor-bearing microparticles and CA19.9: two players in pancreatic cancer-associated thrombosis?, *Br. J. Cancer* **115** (2016) 332–338.; DOI:10.1038/bjc.2016.170

14.A. Bharthuar, A. A. Khorana, A. Hutson, J.-G. Wang, N. S. Key, N. Mackman and R. V. Iyer, Circulating microparticle tissue factor, thromboembolism and survival in pancreaticobiliary cancers, *Thromb. Res.* **132** (2013) 180–184.; DOI:10.1016/j.thromres.2013.06.026

15.M. T. Sartori, A. Della Puppa, A. Ballin, E. Campello, C. M. Radu, G. Saggiorato, D. d'Avella, R. Scienza, G. Cella and P. Simioni, Circulating microparticles of glial origin and tissue factor bearing in high-grade glioma: a potential prothrombotic role, *Thromb. Haemost.* **110** (2013) 378–385.; DOI:10.1160/TH12-12-0957

16.D. Faille, M.-C. Bourrienne, E. de Raucourt, L. de Chaisemartin, V. Granger, R. Lacroix, L. Panicot-Dubois, P. Hammel, P. Lévy, P. Ruszniewski, N. Ajzenberg and V. Rebours, Biomarkers for the risk of thrombosis in pancreatic adenocarcinoma are related to cancer process, *Oncotarget* **9** (2018) 26453–26465.; DOI:10.18632/oncotarget.25458

17.Y. Hisada and N. Mackman, Cancer-associated pathways and biomarkers of venous thrombosis, *Blood* **130** (2017) 1499–1506.; DOI:10.1182/blood-2017-03-743211

18.Y. Hisada and N. Mackman, Measurement of tissue factor activity in extracellular vesicles from human plasma samples, *Res. Pract. Thromb. Haemost.* **3** (2018) 44–48.; DOI:10.1002/rth2.12165

19.S. P. Grover and N. Mackman, Tissue Factor: An Essential Mediator of Hemostasis and Trigger of Thrombosis, *Arterioscler. Thromb. Vasc. Biol.* **38** (2018) 709–725.; DOI:10.1161/ATVBAHA.117.309846

20.R. D. Lee, D. A. Barcel, J. C. Williams, J. G. Wang, J. C. Boles, D. A. Manly, N. S. Key and N. Mackman, Pre-analytical and analytical variables affecting the measurement of plasma-derived microparticle tissue factor activity, *Thromb. Res.* **129** (2012) 80–85.; DOI:10.1016/j.thromres.2011.06.004

21.H. C. Hemker, P. Giesen, R. AlDieri, V. Regnault, E. de Smed, R. Wagenvoord, T. Lecompte and S. Béguin, The Calibrated Automated Thrombogram (CAT): a universal routine test for hyper- and hypocoagulability, *Pathophysiol. Haemost. Thromb.* **32** (2002) 249–253.; DOI:10.1159/000073575

678 22.T. Exner, J. Joseph, J. Low, D. Connor and D. Ma, A new activated factor X-based clotting
679 method with improved specificity for procoagulant phospholipid, *Blood Coagul.*
680 *Fibrinolysis Int. J. Haemost. Thromb.* **14** (2003) 773–779.; DOI:10.1097/00001721-
681 200312000-00015
682 23.R. J. Berckmans, A. Sturk, L. M. van Tienen, M. C. L. Schaap and R. Nieuwland, Cell-
683 derived vesicles exposing coagulant tissue factor in saliva, *Blood* **117** (2011) 3172.;
684 DOI:10.1182/blood-2010-06-290460
685 24.L. Vallier, T. Bouriche, A. Bonifay, C. Judicone, J. Bez, C. Franco, C. Guervilly, Y.
686 Hisada, N. Mackman, R. Houston, P. Poncelet, F. Dignat-George and R. Lacroix,
687 Increasing the sensitivity of the human microvesicle tissue factor activity assay,
688 *Thromb. Res.* **182** (2019) 64–74.; DOI:10.1016/j.thromres.2019.07.011
689 25.R. Linares, S. Tan, C. Gounou, N. Arraud and A. R. Brisson, High-speed centrifugation
690 induces aggregation of extracellular vesicles, *J. Extracell. Vesicles* **4** (2015) 29509–
691 29509.; DOI:10.3402/jev.v4.29509
692 26.Å. Thulin, C. Christersson, J. Alfredsson and A. Siegbahn, Circulating cell-derived
693 microparticles as biomarkers in cardiovascular disease, *Biomark. Med.* **10** (2016)
694 1009–1022.; DOI:10.2217/bmm-2016-0035
695 27.C. Théry, K. W. Witwer, E. Aikawa, M. J. Alcaraz, J. D. Anderson, R. Andriantsitohaina,
696 A. Antoniou, T. Arab, F. Archer, G. K. Atkin-Smith, D. C. Ayre, J.-M. Bach, D.
697 Bachurski, H. Baharvand, L. Balaj, S. Baldacchino, N. N. Bauer, A. A. Baxter, et al.,
698 Minimal information for studies of extracellular vesicles 2018 (MISEV2018): a
699 position statement of the International Society for Extracellular Vesicles and update of
700 the MISEV2014 guidelines, *J. Extracell. Vesicles* **7** (2018) 1535750–1535750.;
701 DOI:10.1080/20013078.2018.1535750

28.E. Roca, R. Lacroix, C. Judicone, S. Laroumagne, S. Robert, S. Cointe, A. Muller, E. Kaspi, P. Roll, A. R. Brisson, C. Tantucci, P. Astoul and F. Dignat-George, Detection of EpCAM-positive microparticles in pleural fluid: A new approach to mini-invasively identify patients with malignant pleural effusions, *Oncotarget* **7** (2015) 3357–3366.; DOI:10.18632/oncotarget.6581

29.P. Poncelet, S. Robert, T. Bouriche, J. Bez, R. Lacroix and F. Dignat-George, Standardized counting of circulating platelet microparticles using currently available flow cytometers and scatter-based triggering: Forward or side scatter?, *Cytometry A* **89** (2016) 148–158.; DOI:10.1002/cyto.a.22685

30.S. Cointe, C. Judicone, S. Robert, M. J. Mooberry, P. Poncelet, M. Wauben, R. Nieuwland, N. S. Key, F. Dignat-George and R. Lacroix, Standardization of microparticle enumeration across different flow cytometry platforms: results of a multicenter collaborative workshop, *J. Thromb. Haemost. JTH* **15** (2017) 187–193.; DOI:10.1111/jth.13514

31.N. S. Key, A. Slungaard, L. Dandelet, S. C. Nelson, C. Moertel, L. A. Styles, F. A. Kuypers and R. R. Bach, Whole Blood Tissue Factor Procoagulant Activity Is Elevated in Patients With Sickle Cell Disease, *Blood* **91** (1998) 4216–4223.; DOI:10.1182/blood.V91.11.4216

32.É. Biró, K. N. Sturk-Maquelin, G. M. T. Vogel, D. G. Meuleman, M. J. Smit, C. E. Hack, A. Sturk and R. Nieuwland, Human cell-derived microparticles promote thrombus formation in vivo in a tissue factor-dependent manner, *J. Thromb. Haemost.* **1** (2003) 2561–2568.; DOI:10.1046/j.1538-7836.2003.00456.x

33.F. Siddiqui, A. Tafur, L. S. Ramacciotti, W. Jeske, D. Hoppensteadt, E. Ramacciotti, O. Iqbal and J. Fareed, Reversal of Factor Xa Inhibitors by Andexanet Alfa May Increase Thrombogenesis Compared to Pretreatment Values, *Clin. Appl. Thromb. Off. J. Int.*

Acad. Clin. Appl. Thromb. **25** (2019) 1076029619863493–1076029619863493.; DOI:10.1177/1076029619863493

34.O. Aras, A. Shet, R. R. Bach, J. L. Hysjulien, A. Slungaard, R. P. Hebbel, G. Escolar, B. Jilma and N. S. Key, Induction of microparticle- and cell-associated intravascular tissue factor in human endotoxemia, *Blood* **103** (2004) 4545–4553.; DOI:10.1182/blood-2003-03-0713

35.M. Y. Konoshenko, E. A. Lekchnov, A. V. Vlassov and P. P. Laktionov, Isolation of Extracellular Vesicles: General Methodologies and Latest Trends, *BioMed Res. Int.* **2018** (2018) 8545347–8545347.; DOI:10.1155/2018/8545347

36.L. M. Doyle and M. Z. Wang, Overview of Extracellular Vesicles, Their Origin, Composition, Purpose, and Methods for Exosome Isolation and Analysis, *Cells* **8** (2019) 727.; DOI:10.3390/cells8070727

37.J. Van Deun, P. Mestdagh, R. Sormunen, V. Cocquyt, K. Vermaelen, J. Vandesompele, M. Bracke, O. De Wever and A. Hendrix, The impact of disparate isolation methods for extracellular vesicles on downstream RNA profiling, *J. Extracell. Vesicles* **3** (2014) 10.3402/jev.v3.24858.; DOI:10.3402/jev.v3.24858

38.R. J. Lobb, M. Becker, S. W. Wen, C. S. F. Wong, A. P. Wiegmans, A. Leimgruber and A. Möller, Optimized exosome isolation protocol for cell culture supernatant and human plasma, *J. Extracell. Vesicles* **4** (2015) 27031–27031.; DOI:10.3402/jev.v4.27031

39.A. Gámez-Valero, M. Monguió-Tortajada, L. Carreras-Planella, M. la Franquesa, K. Beyer and F. E. Borràs, Size-Exclusion Chromatography-based isolation minimally alters Extracellular Vesicles' characteristics compared to precipitating agents, *Sci. Rep.* **6** (2016) 33641–33641.; DOI:10.1038/srep33641

40.A. N. Böing, E. van der Pol, A. E. Grootemaat, F. A. W. Coumans, A. Sturk and R. Nieuwland, Single-step isolation of extracellular vesicles by size-exclusion

chromatography, *J. Extracell. Vesicles* **3** (2014) 10.3402/jev.v3.23430.; DOI:10.3402/jev.v3.23430

41.F. Momen-Heravi, L. Balaj, S. Alian, P.-Y. Mantel, A. E. Halleck, A. J. Trachtenberg, C. E. Soria, S. Oquin, C. M. Bonebreak, E. Saracoglu, J. Skog and W. P. Kuo, Current methods for the isolation of extracellular vesicles, *Biol. Chem.* **394** (2013) 1253–1262.; DOI:10.1515/hsz-2013-0141

42.J. Webber and A. Clayton, How pure are your vesicles?, *J. Extracell. Vesicles* **2** (2013) 10.3402/jev.v2i0.19861.; DOI:10.3402/jev.v2i0.19861

43.T. Baranyai, K. Herczeg, Z. Onódi, I. Voszka, K. Módos, N. Marton, G. Nagy, I. Mäger, M. J. Wood, S. El Andaloussi, Z. Pálinkás, V. Kumar, P. Nagy, Á. Kittel, E. I. Buzás, P. Ferdinandy and Z. Giricz, Isolation of Exosomes from Blood Plasma: Qualitative and Quantitative Comparison of Ultracentrifugation and Size Exclusion Chromatography Methods, *PloS One* **10** (2015) e0145686–e0145686.; DOI:10.1371/journal.pone.0145686

44.A. Morales-Kastresana, T. A. Musich, J. A. Welsh, W. Telford, T. Demberg, J. C. S. Wood, M. Bigos, C. D. Ross, A. Kachynski, A. Dean, E. J. Felton, J. Van Dyke, J. Tigges, V. Toxavidis, D. R. Parks, W. R. Overton, A. H. Kesarwala, G. J. Freeman, et al., High-fidelity detection and sorting of nanoscale vesicles in viral disease and cancer, *J. Extracell. Vesicles* **8** (2019) 1597603.; DOI:10.1080/20013078.2019.1597603

45.A. Liga, A. D. B. Vliegenthart, W. Oosthuyzen, J. W. Dear and M. Kersaudy-Kerhoas, Exosome isolation: a microfluidic road-map, *Lab. Chip* **15** (2015) 2388–2394.; DOI:10.1039/C5LC00240K

46.C. Chen, B.-R. Lin, M.-Y. Hsu and C.-M. Cheng, Paper-based devices for isolation and characterization of extracellular vesicles, *J. Vis. Exp. JoVE* (2015) e52722–e52722.; DOI:10.3791/52722

47.Å. Thulin, J. Yan, M. Åberg, C. Christersson, M. Kamali-Moghaddam and A. Siegbahn, Sensitive and Specific Detection of Platelet-Derived and Tissue Factor-Positive Extracellular Vesicles in Plasma Using Solid-Phase Proximity Ligation Assay, *TH Open Companion J. Thromb. Haemost.* **2** (2018) e250–e260.; DOI:10.1055/s-0038-1667204

48.N. S. Barteneva, E. Fasler-Kan, M. Bernimoulin, J. N. H. Stern, E. D. Ponomarev, L. Duckett and I. A. Vorobjev, Circulating microparticles: square the circle, *BMC Cell Biol.* **14** (2013) 23–23.; DOI:10.1186/1471-2121-14-23

49.D. W. Greening, R. Xu, H. Ji, B. J. Tauro and R. J. Simpson, A protocol for exosome isolation and characterization: evaluation of ultracentrifugation, density-gradient separation, and immunoaffinity capture methods, *Methods Mol. Biol. Clifton NJ* **1295** (2015) 179–209.; DOI:10.1007/978-1-4939-2550-6_15

50.P. Poncelet, B.-F. I and T. Lavabre-Bertrand, Clinical applications of quantitative immunophenotyping., *Immunophenotyping* (January 2000., pp. 105–132). Wiley-Liss.

51.G. J. Ruiz-Delgado, E. Vázquez-Garza, N. Méndez-Ramírez and D. Gómez-Almaguer, Abnormalities in the expression of CD55 and CD59 surface molecules on peripheral blood cells are not specific to paroxysmal nocturnal hemoglobinuria, *Hematology* **14** (2009) 33–37.; DOI:10.1179/102453309X385089

52.H. Rabesandratana, J. P. Toutant, H. Reggio and M. Vidal, Decay-accelerating factor (CD55) and membrane inhibitor of reactive lysis (CD59) are released within exosomes during In vitro maturation of reticulocytes, *Blood* **91** (1998) 2573–2580.; DOI:PMID: 9516159

53.A. de Gassart, C. Géminard, B. Février, G. Raposo and M. Vidal, Lipid raft-associated protein sorting in exosomes, *Blood* **102** (2003) 4336–4344.; DOI:10.1182/blood-2003-03-0871

802 54.F. Collino, M. Pomatto, S. Bruno, R. S. Lindoso, M. Tapparo, W. Sicheng, P. Quesenberry
803 and G. Camussi, Exosome and Microvesicle-Enriched Fractions Isolated from
804 Mesenchymal Stem Cells by Gradient Separation Showed Different Molecular
805 Signatures and Functions on Renal Tubular Epithelial Cells, *Stem Cell Rev. Rep.* **13**
806 (2017) 226–243.; DOI:10.1007/s12015-016-9713-1
807 55.M. Hellum, I. Franco-Lie, R. Øvstebø, T. Hauge and C. E. Henriksson, The effect of corn
808 trypsin inhibitor, anti-tissue factor pathway inhibitor antibodies and phospholipids on
809 microvesicle-associated thrombin generation in patients with pancreatic cancer and
810 healthy controls, *PLOS ONE* **12** (2017) e0184579.;
811 DOI:10.1371/journal.pone.0184579
812 56.K. Tatsumi, S. Antoniak, D. M. Monroe III, A. A. Khorana, N. Mackman and the
813 Subcommittee on Hemostasis and Malignancy, Evaluation of a new commercial assay
814 to measure microparticle tissue factor activity in plasma: communication from the
815 SSC of the ISTH, *J. Thromb. Haemost.* **12** (2014) 1932–1934.;
816 DOI:10.1111/jth.12718
817 57.A. Cvjetkovic, J. Lötvall and C. Lässer, The influence of rotor type and centrifugation time
818 on the yield and purity of extracellular vesicles, *J. Extracell. Vesicles* **3** (2014) 23111.;
819 DOI:10.3402/jev.v3.23111
820 58.S. Cointe, K. Harti Souab, T. Bouriche, L. Vallier, A. Bonifay, C. Judicone, S. Robert, R.
821 Armand, P. Poncelet, J. Albanese, F. Dignat-George and R. Lacroix, A new assay to
822 evaluate microvesicle plasmin generation capacity: validation in disease with
823 fibrinolysis imbalance, *J. Extracell. Vesicles* **7** (2018) 1494482.;
824 DOI:10.1080/20013078.2018.1494482
825 59.K. Meszaros, S. Aberle, R. Dedrick, R. Machovich, A. Horwitz, C. Birr, G. Theofan and J.
826 Parent, Monocyte tissue factor induction by lipopolysaccharide (LPS): dependence on

LPS-binding protein and CD14, and inhibition by a recombinant fragment of bactericidal/permeability-increasing protein, *Blood* **83** (1994) 2516.; Retrieved from http://www.bloodjournal.org/content/83/9/2516.abstract

60.A. N. Barclay, M. H. Brown, S. K. A. Law, A. J. McKnight, M. G. Tomlinson and P. A. van der Merwe, - CD61, In A. N. Barclay, M. H. Brown, S. K. A. Law, A. J. McKnight, M. G. Tomlinson, & P. A. van der Merwe (Eds.), *Leucoc. Antigen FactsBook* (pp. 293–294). San Diego: Academic Press.; DOI:10.1016/B978-012078185-0/50500-X

61.S. A. Melo, L. B. Luecke, C. Kahlert, A. F. Fernandez, S. T. Gammon, J. Kaye, V. S. LeBleu, E. A. Mittendorf, J. Weitz, N. Rahbari, C. Reissfelder, C. Pilarsky, M. F. Fraga, D. Piwnica-Worms and R. Kalluri, Glypican-1 identifies cancer exosomes and detects early pancreatic cancer, *Nature* **523** (2015) 177–182.; DOI:10.1038/nature14581

62.M. Takao, Y. Nagai, M. Ito and T. Ohba, Flow cytometric quantitation of EpCAM-positive extracellular vesicles by immunomagnetic separation and phospholipid staining method, *Genes Cells* **23** (2018) 963–973.; DOI:10.1111/gtc.12645

63.C. Campos-Silva, H. Suárez, R. Jara-Acevedo, E. Linares-Espinós, L. Martinez-Piñeiro, M. Yáñez-Mó and M. Valés-Gómez, High sensitivity detection of extracellular vesicles immune-captured from urine by conventional flow cytometry, *Sci. Rep.* **9** (2019) 2042.; DOI:10.1038/s41598-019-38516-8

64.H. Shao, J. Chung, K. Lee, L. Balaj, C. Min, B. S. Carter, F. H. Hochberg, X. O. Breakefield, H. Lee and R. Weissleder, Chip-based analysis of exosomal mRNA mediating drug resistance in glioblastoma, *Nat. Commun.* **6** (2015) 6999–6999.; DOI:10.1038/ncomms7999

851 65.P. Sharma, S. Ludwig, L. Muller, C. S. Hong, J. M. Kirkwood, S. Ferrone and T. L.
852 Whiteside, Immunoaffinity-based isolation of melanoma cell-derived exosomes from
853 plasma of patients with melanoma, *J. Extracell. Vesicles* **7** (2018) 1435138.;
854 DOI:10.1080/20013078.2018.1435138
855 66.Z. Zhao, Y. Yang, Y. Zeng and M. He, A microfluidic ExoSearch chip for multiplexed
856 exosome detection towards blood-based ovarian cancer diagnosis, *Lab. Chip* **16** (2016)
857 489–496.; DOI:10.1039/c5lc01117e
858

A

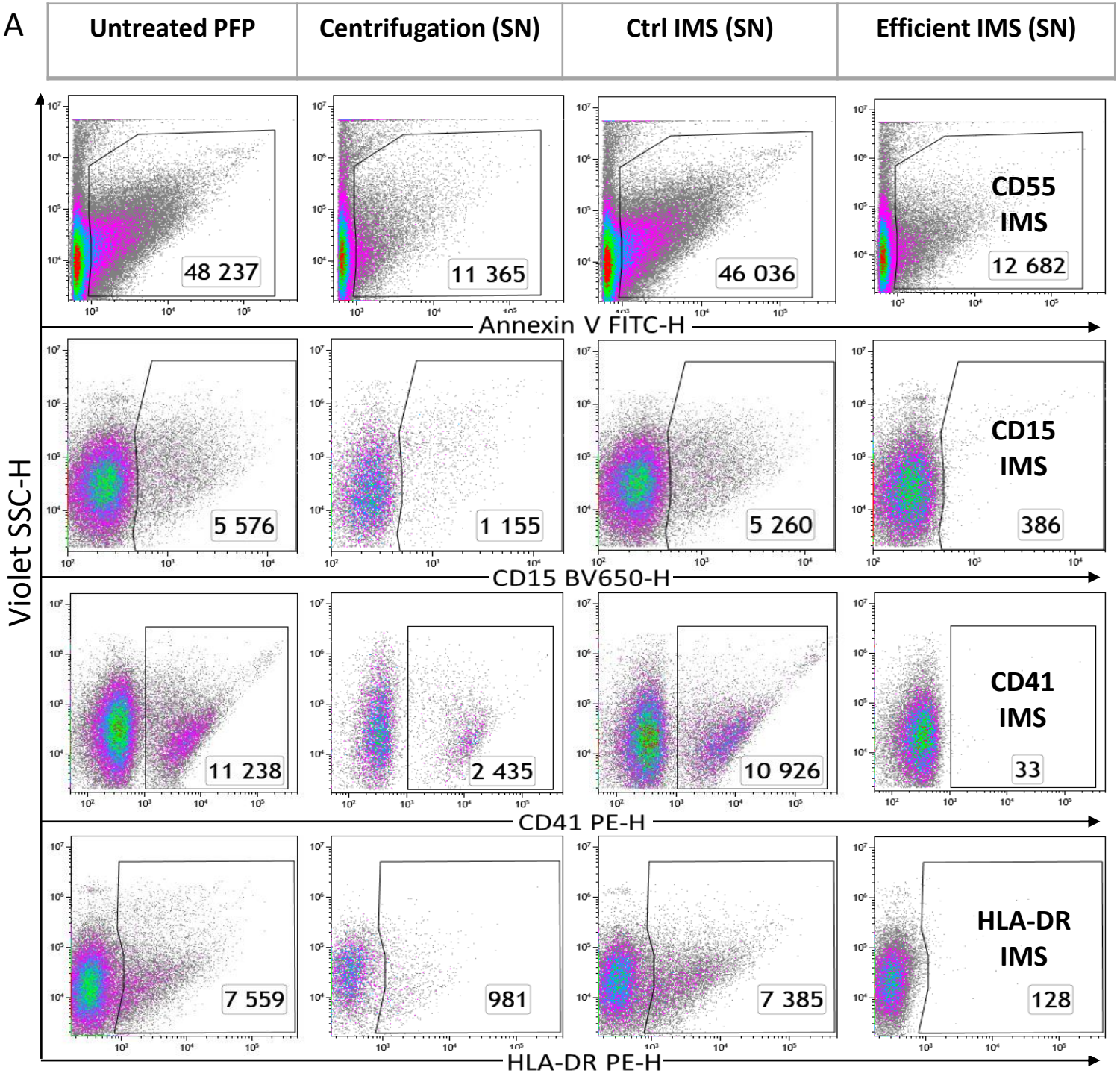
Untreated PFP
Centrifugation (SN)
Ctrl IMS (SN)
Efficient IMS (SN)
48 237
11 365
46 036
CD55 IMS
12 682
Annexin V FITC-H
5 576
1 155
5 260
CD15 IMS
386
CD15 BV650-H
11 238
2 435
10 926
CD41 IMS
33
CD41 PE-H
7 559
981
7 385
HLA-DR IMS
128
HLA-DR PE-H
Violet SSC-H

B

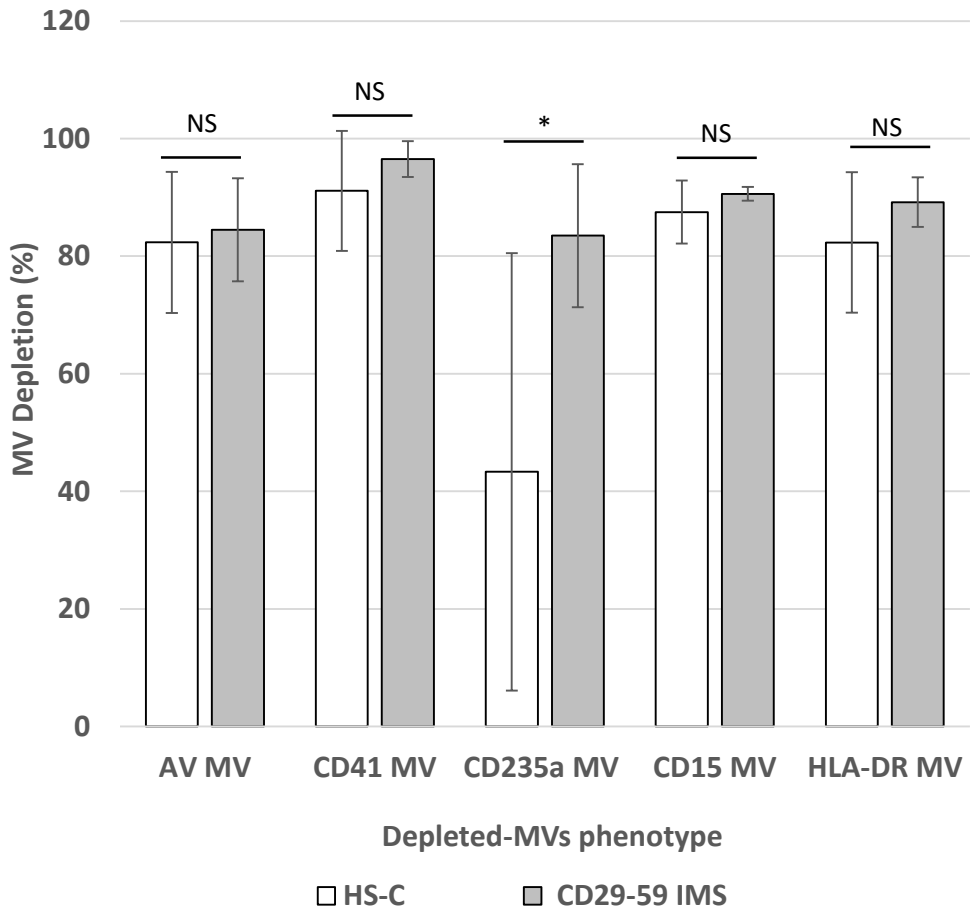
120
100
80
60
40
20
0
MV Depletion (%)
NS
NS
*
NS
NS
AV MV
CD41 MV
CD235a MV
CD15 MV
HLA-DR MV
Depleted-MVs phenotype
HS-C
CD29-59 IMS

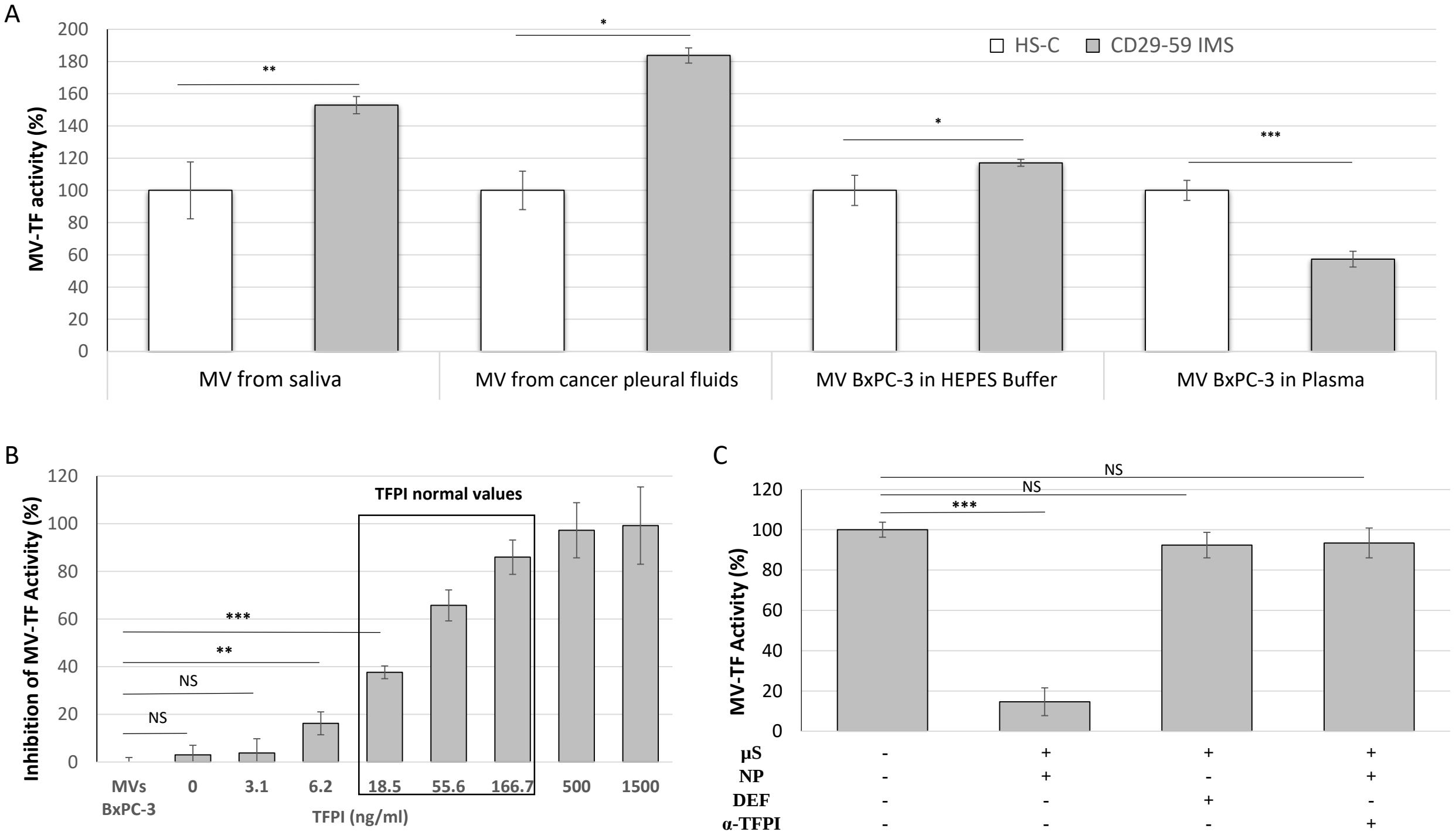
A
HS-C
CD29-59 IMS
MV-TF activity (%)
200
180
160
140
120
100
80
60
40
20
0
**
*
*
***
MV from saliva
MV from cancer pleural fluids
MV BxPC-3 in HEPES Buffer
MV BxPC-3 in Plasma
B
Inhibition of MV-TF Activity (%)
120
100
80
60
40
20
0
TFPI normal values
***
**
NS
NS
MVs BxPC-3
0
3.1
6.2
18.5
55.6
166.7
500
1500
TFPI (ng/ml)
C
MV-TF Activity (%)
120
100
80
60
40
20
0
NS
NS
***
μS - + + +
NP - + - +
DEF - - + -
α-TFPI - - - +

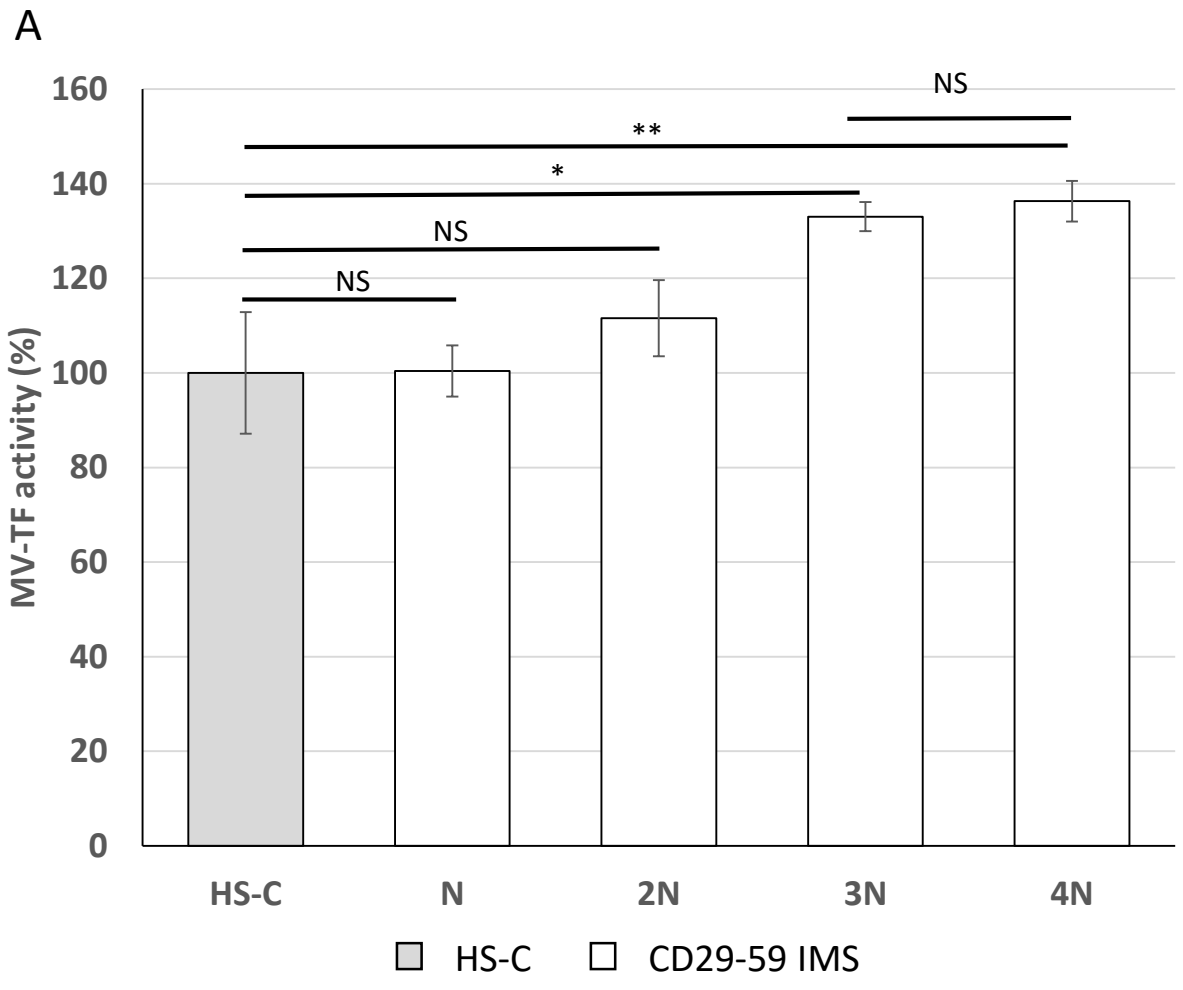
A
160
140
120
100
80
60
40
20
0
MV-TF activity (%)
NS
**
*
NS
NS
HS-C
N
2N
3N
4N
HS-C
CD29-59 IMS

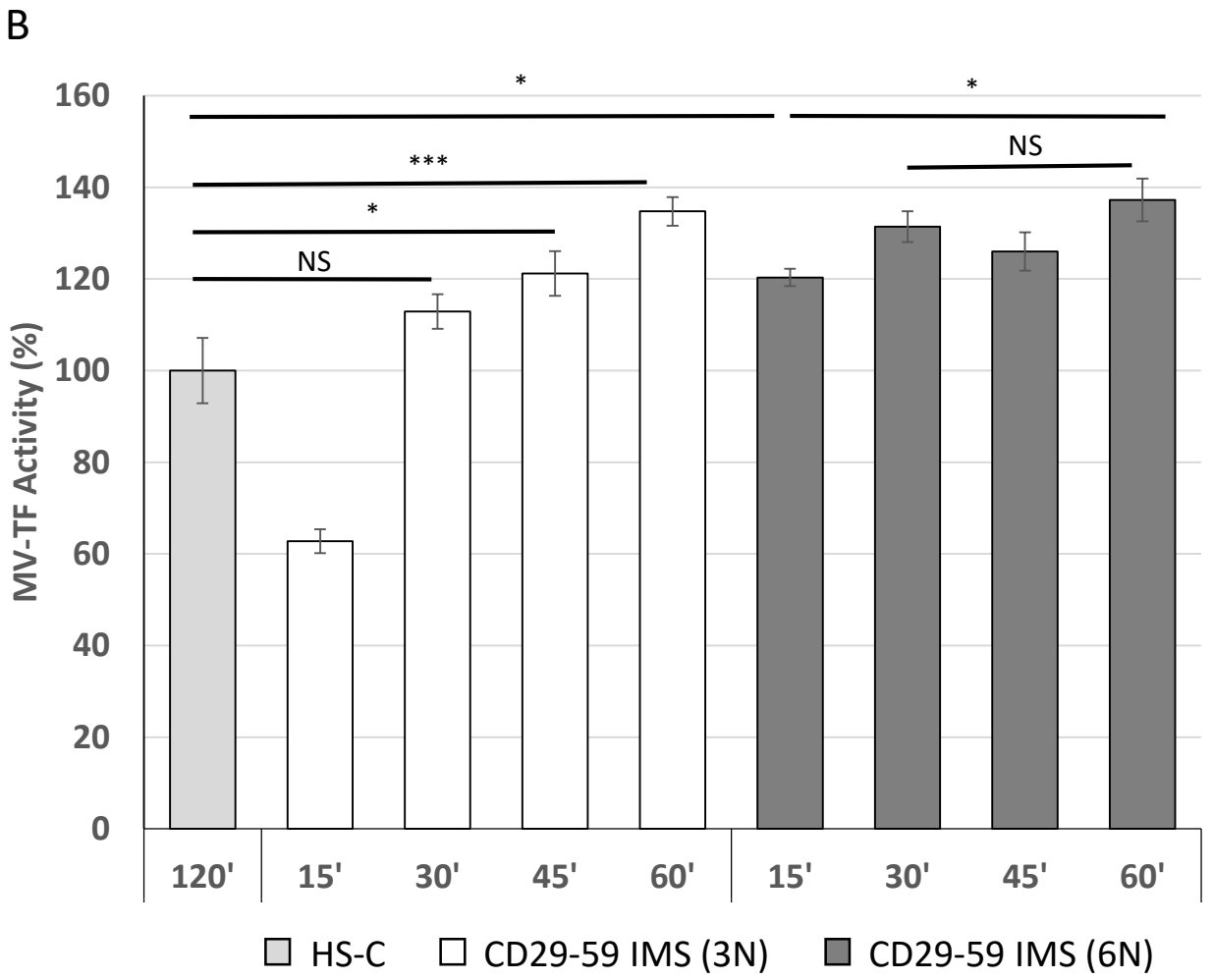
B
160
140
120
100
80
60
40
20
0
MV-TF Activity (%)
*
*
***
NS
*
NS
120'
15'
30'
45'
60'
15'
30'
45'
60'
HS-C
CD29-59 IMS (3N)
CD29-59 IMS (6N)

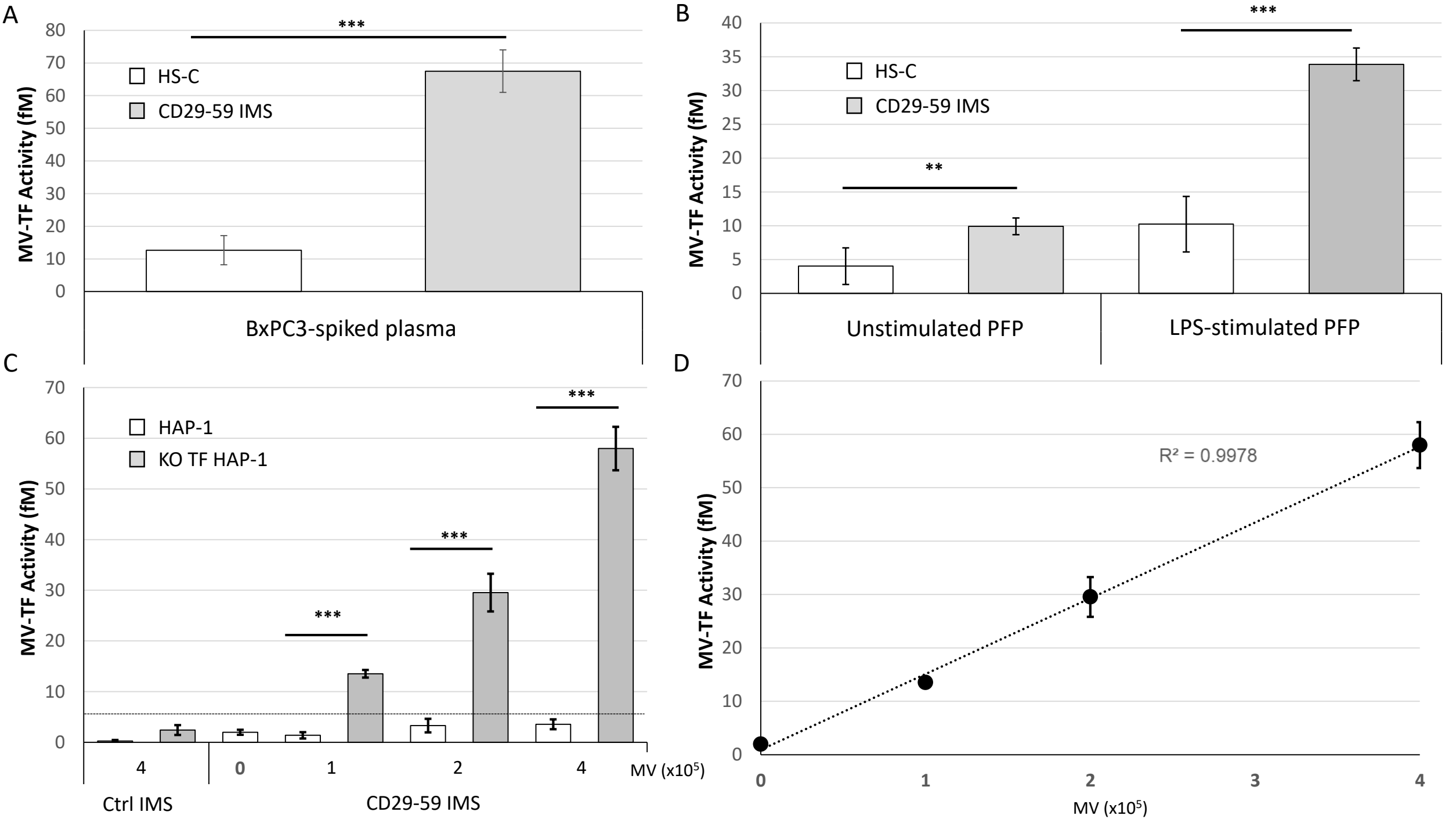
A
MV-TF Activity (fM)
HS-C
CD29-59 IMS
***
BxPC3-spiked plasma
B
MV-TF Activity (fM)
HS-C
CD29-59 IMS
**
***
Unstimulated PFP
LPS-stimulated PFP
C
MV-TF Activity (fM)
HAP-1
KO TF HAP-1
***
***
***
4
0
1
2
4
MV (x10⁵)
Ctrl IMS
CD29-59 IMS
D
MV-TF Activity (fM)
R² = 0.9978
0
1
2
3
4
MV (x10⁵)

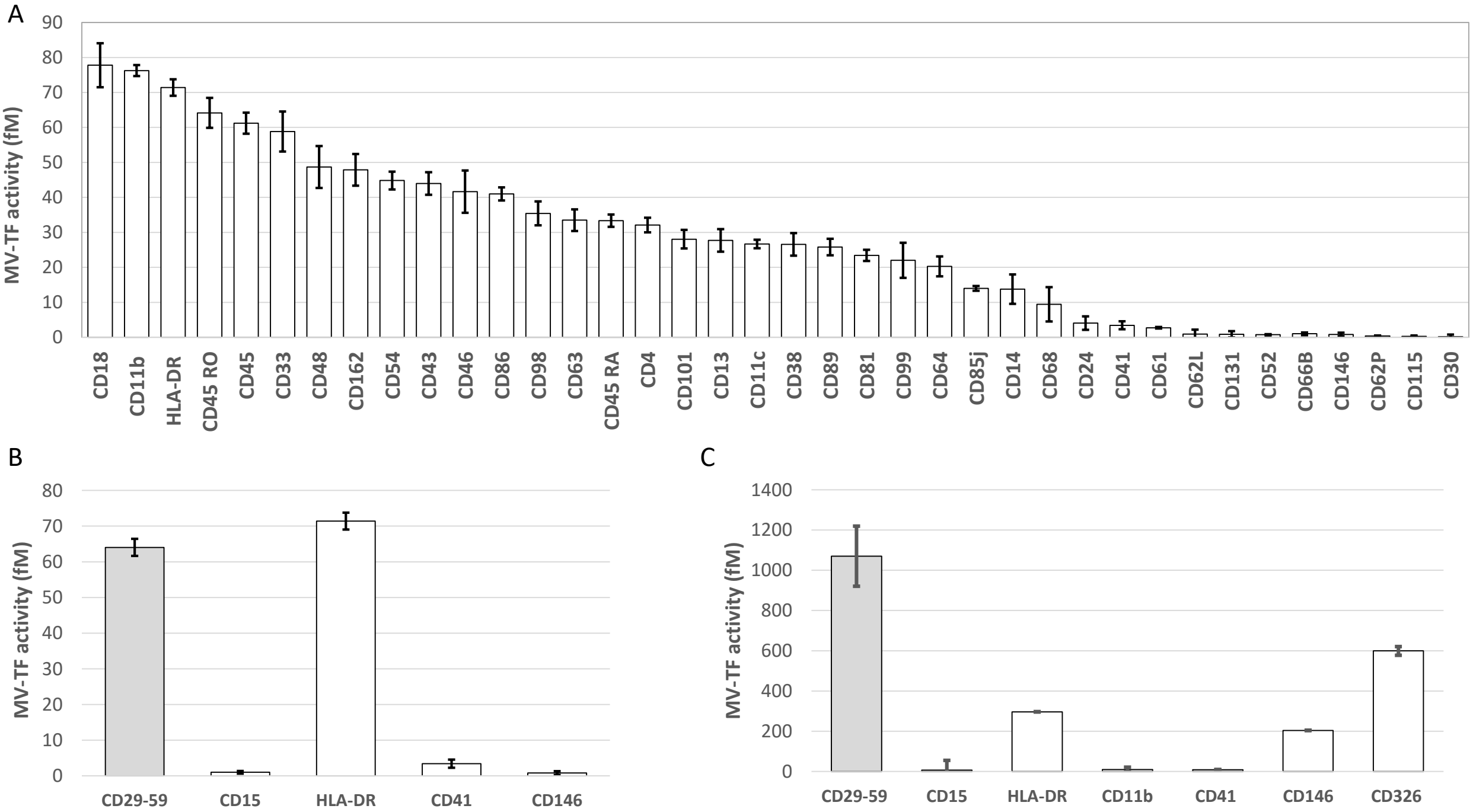
A
MV-TF activity (fM)
0
10
20
30
40
50
60
70
80
90
CD18
CD11b
HLA-DR
CD45 RO
CD45
CD33
CD48
CD162
CD54
CD43
CD46
CD86
CD98
CD63
CD45 RA
CD4
CD101
CD13
CD11c
CD38
CD89
CD81
CD99
CD64
CD85j
CD14
CD68
CD24
CD41
CD61
CD62L
CD131
CD52
CD66B
CD146
CD62P
CD115
CD30
B
MV-TF activity (fM)
0
10
20
30
40
50
60
70
80
CD29-59
CD15
HLA-DR
CD41
CD146
C
MV-TF activity (fM)
0
200
400
600
800
1000
1200
1400
CD29-59
CD15
HLA-DR
CD11b
CD41
CD146
CD326